INTERCALATION AND EXPANSION OF NOVEL GRAPHITE BISULFATE COMPOUNDS

A. Longo, G. Carotenuto*

Institute for Polymers, Composites and Biomaterials;
National Research Council,
UOS Napoli/Portici
Piazzale E. Fermi 1
80055 Portici, Naples
Italy

angela.longo@cnr.it

S. De Nicola, C. Camerlingo

SPIN;
National Research Council
Complesso Universitario
Monte Sant'Angelo
Via Cinthia
80126 Naples,
Italy

E. Pugliese, M. Ciofini, M. Locatelli, A. Lapucci, R. Meucci

National Institute of Optics;
National Research Council
Largo E. Fermi 6
50126 Florence,
Italy

Abstract
Graphite intercalation compounds are of interest for graphene production and represent examples that allow to study reactions in confined conditions. In this work, graphite bisulfate has been prepared by intercalating sulfuric acid molecules into graphite flakes in presence of either periodate (IO_4^-) or chlorate (ClO_3^-) oxidizing agents. The obtained graphite intercalation compounds exhibit very high thermal expansion capability. The intercalation and expansion processes have been investigated by comparing thermogravimetric analysis, scanning electron microscopy and micro-Raman spectroscopy results of these graphite bisulfate compounds whit that of a commercial one. Laser-induced expansion of intercalated graphite bisulfate compounds was observed in real time by thermal and visible high speed camera video.

Key words
Graphite intercalation compounds, graphite bisulfate, laser-induced expansion, micro-Raman spectroscopy, infrared camera video.

1 Introduction

Graphite intercalation compounds (GICs) are useful exotic materials made of graphite flakes embedding small molecules or metal ions between the graphene sheets [1]. GICs can be used for sensing/biosensing as other nanosized carbon materials since their electronic properties are highly tunable in many ways by chemical or electrical manipulations. Highly efficient graphene quantum dots emitting near the UV-Vis range (λ_{em}=400 nm) have been fabricated from GICs using potassium-sodium tartrate as intercalant [2]. GICs obtained by the introduction of certain metal or small molecules between the graphite layers, such as in KC_8, have been shown to exhibit remarkable superconducting properties [3]. In addition, they are being currently used for producing other high-quality *quasi*-graphene materials (e.g. few-layers graphene, graphite nanoplatelets, etc.) [4]. Alternative approaches for the synthesis of graphene (e.g., chemical vapor deposition on copper, epitaxial growth, etc.) lead to products with lower electronic performance (reduced electron mobility) [5-8]. Typically, the starting material for these *quasi*-graphene materials is graphite bisulfate (i.e. GICs where bisulfate ions and H_2SO_4 molecules alternate with graphene sheets) originally prepared by Schafheutl [9] and Brodie [10]. These kind of GICs are able to expand by thermal shock, giving rise to a high disordered, warm-like graphene-based structure, named expanded graphite. Nowadays, this kind of chemical compound is commercially available (by companies like Faima, Asbury, etc.) and it always consists of graphite bisulfate obtained by treating pure graphite flakes of different size distribution with alkaline metal nitrate or permanganate solution in absolute sulfuric acid. In addition, limited studies are available in the literature about the optimal auxiliary reagent (oxidizing agent), although a variety of chemical compounds were indicated in the original recipes [9-11].

Here, we report the use of two strong oxidizers (IO_4^- and ClO_3^-), which leads to a high expandable graphite bisulfates. The expansion ability of the achieved graphite bisulfate compounds has been compared to that of a commercial graphite bisulfate, provided by Faima. The samples have been characterized by thermogravimetric analysis (TGA), scanning electron microscopy (SEM) and micro-Raman spectroscopy. We have also investigated a simple and fast technique for graphite bisulfate thermal expansion induced by a

continuous-wave infrared laser at ambient pressure and the process was analyzed in real time by thermal and visible high speed camera video.

2 Experimental parts

The graphite bisulphate compounds were synthesized by treating graphite flakes with H_2SO_4/oxidizing agent mixture (9:1 by volume ratio). In particular, the use of two alternative strong oxidizers, i.e. $NaIO_4$ and $NaClO_3$, was analyzed.

Constant quantities of graphite flakes (2g, Aldrich, >100 mesh), sulphuric acid (40mL), and oxidizing agent were used. All reactants were placed in a glass-flask and a slow air-bubbling was applied to homogenize the system during the reaction. A thermostatic bath was used to assure a uniform and controlled process temperature. Cold deionized water was added to the reactive mixture after 1 hour to stop the reaction. The obtained product was washed with water by vacuum filtration.

The thermal expansion threshold of the different intercalation compounds was measured by thermogravimetric analysis (TGA), using a TA Q5000 instrument with a heating rate of 10 °C min^{-1} under fluxing nitrogen.

Micro-Raman (μ-RS) spectroscopy was used to analyze the chemical structure of pure graphite and "as-prepared" graphite bisulphate compounds. A Jobin-Yvon system from Horiba ISA, with a TriAx 180 monochromator, equipped with a liquid nitrogen cooled charge-coupled detector was used for the μ-RS measurements. The grating of 1800 grooves/mm allows a final spectral resolution of 4cm^{-1}. The spectra were recorded in air at room temperature using a 17mW He-Ne laser source (λ=632.8nm). The spectrum accumulation time was 120s. The laser light was focused to a 2μm spot size on the sample through an Olympus microscope with 100× optical objective. The spectra obtained were analyzed in terms of convoluted Lorentzian functions by using a best-fitting routine.

Structural and morphological characterizations of graphite bisulfate compounds before and after intercalation and after expansion were obtained by SEM using a FEI Quanta 200 FEG equipped with an Oxford Inca Energy System 250.

A continuous-wave infrared laser induced thermal expansion process was performed on graphite bisulfate compounds provided by Faima. A medium-power IR diode pumped laser source (Yitterbium laser, YLR-100-SM-AC by IGP Photonics) emitting at a wavelength λ=1.07μm and a tunable output power from 10 to 100W was used to induce the thermal expansion process. The output power was controlled by varying the current of the pumping diode laser and using an 80/20 beam splitter. The radiation dose on each grain was accurately measured by means of a power meter. In the irradiation process, the laser power on the grain was gradually increased in steps of 0.2W from an initial value of 4W up to the grain explosion. The beam waist was 4mm, resulting in a radiation dose of 16W/cm2 at the surface of the grain. The beam waist was larger than the typical size of the grain (of the order of 0.5mm).

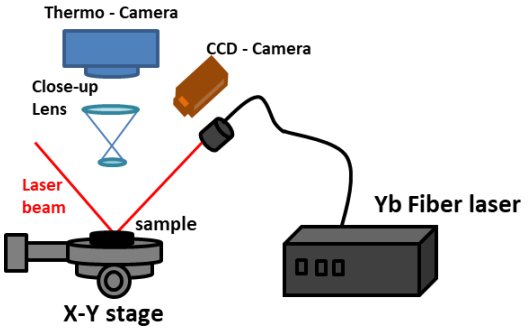

Figure 1 Experimental setup for monitoring the laser induced thermal exfoliation process

Due to the small size of the irradiated grains, a high resolution microscope, equipped with a pyroelectric camera (Spiricon Pyrocam III) and a high-speed visible video camera were used. Figure 1 shows a scheme of the experimental setup employed for monitoring the laser-induced thermal expansion process. The system was specifically designed to allow for simultaneously recording both visible and IR images and correlating the evolution of the grain expansion with the temporal behavior of the thermal field during the laser irradiation. The thermal response of the system was calibrated by relating the intensity levels of the thermos-camera to the temperature measurements. The process was monitored in the mid-IR region (8−12μm) in order to separate the relatively weak thermal emission of the grains from the large amount of scattered laser radiation. IR videos were recorded up to a maximum rate of 24frames/s by using a Ge close-up lens system. Visible videos were recorded at a high rate (250frames/s) by a camera equipped with a macrolens.

3 Results and discussion

Dynamic thermogravimetric analysis provides an important method for investigating kinetics of the thermal decomposition/expansion of graphite intercalation compounds [12].

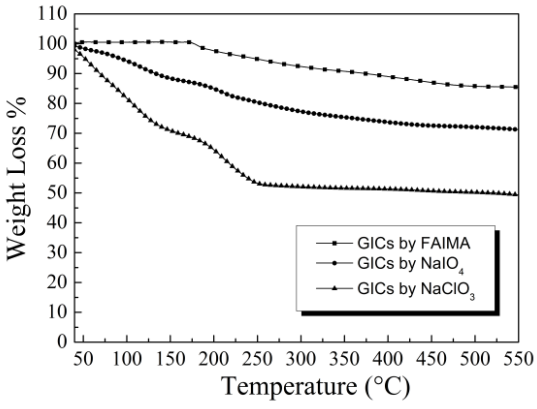

Figure 2 TGA thermograms of graphite bisulfates

The thermogravimetric behavior of our samples is shown in Figure 2. TGA runs from 40°C to 550°C at a heating rate of 10°C min-1. During the thermal treatment, the expansion phenomenon of GICs occurs [13] and intercalating agent and graphite react in confined conditions [14-18] according to the following scheme [19]

$$C + 2\,H_2SO_4 \rightarrow CO_2 + 2SO_2 + 2H_2O$$

The chemical reaction results in release of gases during the expansion: carbon dioxide, sulfur dioxide, and water vapor. The weight loss, due to the gases released, can be clearly seen in the Figure 2 for the considered samples. TGA thermograms show that the expansion process starts at approximately 150°C for all samples. The maximum weight loss occurred for the GICs by $NaClO_3$ and was an indication of the higher intercalation of the graphite.

The μ-RS spectra obtained from the GICs are reported in Figure 3 and compared with spectrum of pure graphite. In Figure 3(a) the spectrum region in the wavenumber range of 1200-1850cm^{-1} is considered where a prominent peak (designated as G mode) is expected for graphite at about 1582cm^{-1}.

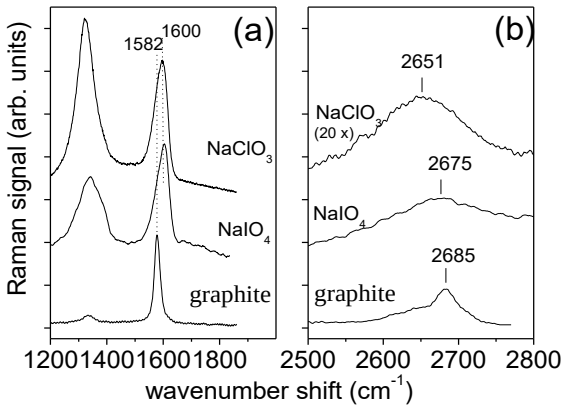

Figure 3 Micro-Raman spectra of graphite intercalated compounds in the wavenumber range of 1200-1850cm^{-1} (a) and 2500-2800cm^{-1}(b).The spectra are shifted arbitrarily along the y-axis. The dotted lines indicate the spectral position of the main components observed for the G mode (a) and the 2D mode (b) peak, respectively.

This peak is clearly visible in the spectrum of graphite and in the GICs spectra, even if the peak are broader and their centers are slightly shifted to a higher wavenumber values. A more accurate analysis reveals that in the case of bisulfates the G mode is adequately fitted by the convolution of two components, one close to the G mode position of pristine graphite assigned to block of not intercalated graphite layers, and another mode at about 1600cm^{-1}, assigned to graphene layers next to an intercalant layer [20]. Two dotted lines indicate the positions of these two modes in Figure 3(a). The Raman mode at about 1332cm^{-1}(D mode) manifests the occurrence of defects in the lattice, and it is significantly stronger in the graphite bisulfate samples than in pristine graphite, presumably related to the intercalated structure. The Raman spectra in the wavenumber range of 2500-2800cm^{-1} are reported in Figure 3(b). For each sample, the scale used of y-axes is the same that the one used in Figure 3(a). In this spectral region, graphite is characterized by a broad peak (designed as 2D mode) centered at about 2685cm^{-1}. Besides the pristine graphite 2D mode (at 2685cm^{-1}), the fit of the experimental data imply the occurrence of a Raman component at about 2648cm^{-1} as prevalent mode in bisulfate samples obtained using $NaIO_4$ and $NaClO_3$ as oxidizers. The Raman band position results shifted to lower wavenumber values (see Figure 3(b)), with respect to pristine graphite as in the case of graphene. These data confirm the occurrence of a large intercalation configuration in the $NaIO_4$ and $NaClO_3$ systems, because the Raman signal is mainly generated by almost monolayers of graphene (intercalated graphite with low number of stages). Raman data are consistent with a better intercalation of GICs obtained by using $NaClO_3$ as oxidizing agent, in agreement with the thermogravimetric results.

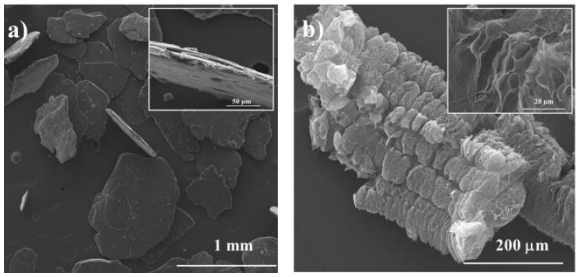

Figure 4 SEM-micrographs after a) and before b) of graphite bisulfate by Faima expansion

The morphology of graphite flakes before and after the expansion process has been investigated by comparing SEM-micrographs of different GICs. Figure 4(a) shows the SEM micrographs of graphite bisulfate grains as received from Faima. It can be clearly seen that the grains are disc-like platelets. An average thickness of 25±1.2μm and size 500±62μm (±SD) were obtained from measurements made on 20 platelets. Figure 4(b) shows the SEM micrographs of graphite bisulfate grains after expansion. It is noticeable the unidirectional expansion induced by the laser, resulting in a sort of worm-like filament, i.e., a long, porous, deformed cylinder-like structure.

At higher magnification (see the inset) scanning electron microscopy shows the full expansion between each layer of the expanded structure and the presence of open channels or cavities. Physically the number, the size and the distribution of such cavities along the worm like structure is expected to depend on the intercalate compounds and the heating rate [21-23].

Figure 5(a) and 5(b) show SEM images of GICs obtained from $NaClO_3$ and $NaIO_4$, respectively. By comparing the morphology of the samples we see that

GICs obtained by using $NaClO_3$ as oxidizing agent exhibits stronger intercalation whereas there is a slight erosion of the flakes boundaries of the GICs by $NaIO_4$ and a less pronounced layer separation (fig. 5(b)).

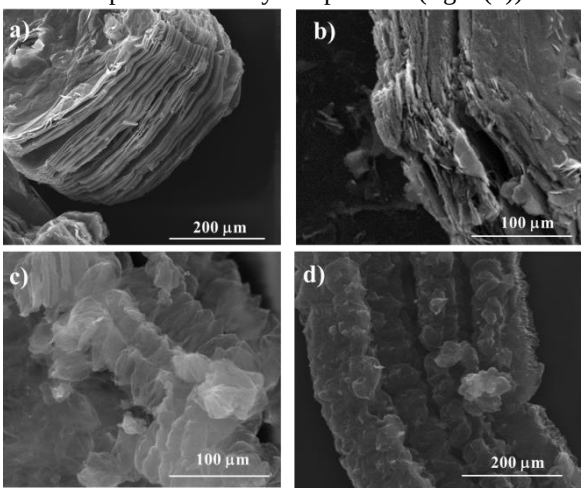

Figure 5 SEM-micrographs after and before expansion process of graphite bisulfate by $NaCl_3$ a), c) and $NaIO_4$ b), d) respectively.

After thermal expansion the SEM micrographs of both samples (see Figure 5(c), 5(d)) show that the expanded samples have a wormlike shape with a lot of pores and defects. This result represents a confirmation of the obtained intercalation during the preparation of samples.

The thermal behavior during expansion process was investigated by image analysis of frames sequences recorded by the infrared video camera. Figure 6(a) shows a sequence of thermal images recorded at different time during the grain explosion process. The temperature field changes significantly during the laser irradiation and the temporal evolution of thermal images shows clearly that the temperature across the grain rises very quickly. The bright red area in the IR images corresponds to the high temperature hot spot across the grain volume. The frame sequence also shows the external region surrounding the hot grain, which becomes colder as the grain expansion process proceeds. This region corresponds to spatial distribution of the temperature field of the gas mixture (i.e. H_2O, CO_2, and SO_2) which are released during the laser induced explosion of the grain. The typical temperature evolution of an irradiated flake over time is shown in figure 6(b). The temperature profile was obtained by averaging the spatial distribution of the temperature across the bright red area and repeating this procedure for each recorded frame sequence. At the beginning of the heating process the temperature of the flake rises slowly until a critical threshold is reached and the chemical reaction is activated. The experimental data show that once the reaction starts, there is a quick rise in temperature from the threshold value of ca. 140°C to a peak value of ca. 350°C which is reached in less than 3s from the beginning of the laser irradiation process, after which the temperature starts decreasing slowly, towards the thermal equilibrium. To improve the accuracy in the determination of the temperature threshold, several measurements were performed on the set of 24 flakes under the same irradiation condition.

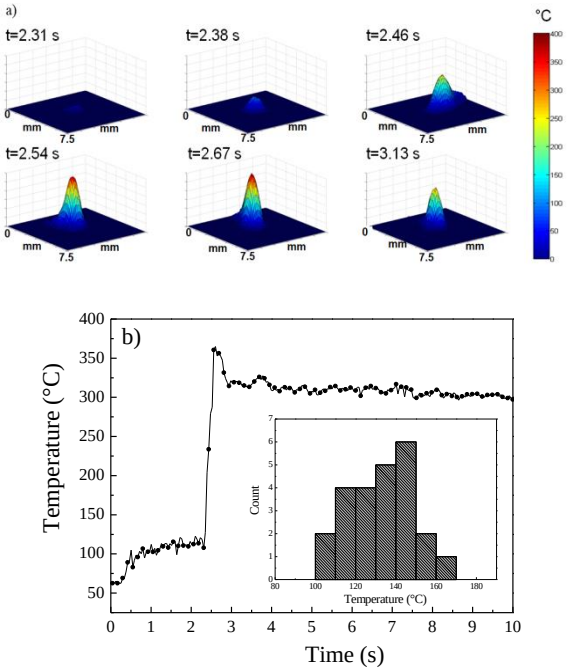

Figure 6 (a) Series of thermal images recorded at different times during the laser-induced expansion of single grain (7.5 × 7.5mm field of view). (b) Typical evolution over the time of the temperature of a single grain exposed to the infrared laser. The inset: histogram of the threshold temperature measurements performed on 24 graphite flakes irradiated under the same conditions.

The inset in Figure 6(b) shows the histogram of the threshold temperature measurements.

The temperature threshold was found to depend on the grain size and its heat dissipation capability at the irradiated zone. A threshold temperature of 140±12°C was obtained.

4 Conclusions

A convenient chemical route, for synthesizing graphite bisulfate compounds based on two uncommon oxidizing agents: $NaClO_3$ and $NaIO_4$, has been developed. Micro-Raman spectroscopy has shown that the obtained intercalation compounds exhibit a high intercalation degree, which is consistent with the weight loss data from the thermogravimetric analysis. Graphite bisulfate thermal expansion by a continuous-wave infrared laser-assisted technique has been monitored using high speed thermal and visible camera video. A temperature threshold expansion was found, with a transition at ca. 140°C followed by formation of a worm-like structure, caused deformed by the gas produced during the laser irradiation.

Acknowledgements

The authors are grateful to Maria Cristina Del Barone from Laboratory of Electron Microscopy "LaMEST" of IPCB-CNR for SEM analysis.

References

[1] Ray S, "Applications of Graphene and Graphene-Oxide based Nanomaterials" Micro and Nano Technologies, 2015 William Andrew – Elsevier.

[2] S. H. Song, M.-H. Jang, J. Chung, S. H. Jin, B. H.Kim, S.-H. Hur, S. Yoo, Y.-H Cho and S. Jeon, (2014), Highly Efficient Light-Emitting Diode of Graphene Quantum Dots Fabricated from Graphite Intercalation Compounds. Advanced Optical Materials, 2: 1016–1023.

[3] E. Weller Thomas, Ellerby Mark, S. Saxena Siddharth, P. Smith Robert and T. Skipper Neal, (2005) Superconductivity in the Intercalated Graphite Compounds C6Yb and C6Ca. Nature Physics 1: 39.

[4] Yoshida, A (1991). Exfoliated graphite from various intercalation compounds. Carbon Vol. 29. No. 8. pp. 1227-1231.

[5] Emtsev, K. V. (2009). Towards wafer-size graphene layers by atmospheric pressure graphitization of silicon carbide. Nat. Mater. 8, 203–207.

[6] Berger, C. (2006). Electronic confinement and coherence in patterned epitaxial graphene. Science 312, 1191–1196.

[7] Sutter, P. W. (2008). Epitaxial graphene on ruthenium. Nat. Mater. 7, 406–411.

[8] Lee, J. H. (2014) Wafer-scale growth of single-crystal monolayer graphene on reusable hydrogen-terminated germanium. Science 344, 286–289.

[9] C. Schafheutl (1840), Ueber die Verbindungen des Kohlenstoffes mit Silicium, Eisen und anderen Metallen, welche die verschiedenen Gallungen von Roheisen, Stahl und Schmiedeeisen bilden, J. Prakt. Chem. 21 129-157.

[10] B. Brodie (1855), Note sur un nouveau procédé pour la purification et la désagrégation du graphite, Ann.Chem. Physique 45 351-352.

[11] U. Hofman W. Rüdorff (1938) The formation of salts from graphite by strong acid, Transaction of Faraday Journal 34, 1017-1021.

[12] H. Ren, F-Y Kang, Q-j Jiao, Q-Z Cui (2006) Kinetics of the thermal decomposition of intercalation compounds during exfoliation. New Carbon Materials, 21, 315.

[13] D.D.L. Chung, (1987) Review exfoliation of graphite, J. of Materials Sci. 22, 4190-4198.

[14] E.E. Santito, A.M. George, M. Sliwinsksa-Bartkowiak, M. Buongiorno Nardelli, K.E. Gubbins (2005) Effect of Confinement on Chemical Reactions. Adsorption, 11(Suppl.1), 349.

[15] X. Pan, X. Bao (2011) The Effects of Confinement inside Carbon Nanotubes on Catalysis, Acc. Chem. Res. 44(8), 553.

[16] J. M. Thomas, R. Raja (2008) Exploiting Nanospace for Asymmetric Catalysis: Confinement of Immobilized, Single-Site Chiral Catalysts Enhances Enantioselectivity, Acc. Chem. Res. 41(6), 708.

[17] R. Mu, Q. Fu, L. Jin, L. Yu, G. Fang, D. Tan, X. Bao (2012) Visualizing Chemical Reactions Confined under Graphene. Angew. Chem. Int. Ed. 51, 4856.

[18] G. Carotenuto, A. Longo, L. Nicolais, S. De Nicola, E. Pugliese, M. Ciofini, M. Locatelli, A. Lapucci, R. Meucci (2015) "Laser-Induced Thermal Expansion of H_2SO_4-Intercalated Graphite Lattice". The Journal of Physical Chemistry C, 119(28): 15942-15947.

[19] C. Camino, S. Duquesne, R. Delobel, B. Eling, C. Lindsay, T. Roels. Chapter 8: Mechanism of expandable graphite fire retardant action in polyurethanes. in Fires and Polymer: Materials and solution for hazard prevention. ACS publisher DC Washingtonh, 2001;90 (symposium serie No. 797).

[20] M. Salvatore, G. Carotenuto, S. De Nicola, C. Camerlingo, V. Ambrogi, C. Carfagna, (2017) Synthesis and Characterization of Highly Intercalated Graphite Bisulfate, Nanoscale Res letters 12, 167.

[21] A. Yoshida, Y. Hishiyama, M. Inagaki (1991) Exfoliated Graphite from Various Intercalation Compounds. Carbon, 29, 1227.

[22] I. M. Yurkovskii, T.Y. Smironova, L.S. Malei (1986) Structural features of the exfoliated graphite. Khim. Tverd. Topl. 1,127.

[23] M. Inagaki, T. Suwa (2201) Pore structure analysis of exfoliated graphite using image processing of scanning electron micro graphs. Carbon 39:9, 15.